

Frustrated Bose-Einstein condensates with non-collinear orbital ordering

Zi Cai,^{1,*} Yu Wang,^{2,†} and Congjun Wu^{1,2}

¹*Department of Physics, University of California, San Diego, CA92093*

²*School of Physics and Technology, Wuhan University, Wuhan 430072, China*

We investigate the unconventional Bose-Einstein condensations with the orbital degree of freedom in the 3D cubic optical lattice, which gives rise to various exotic features absent in conventional scalar and spinor Bose-Einstein condensations. Orbital angular momentum moments are formed on lattice sites breaking time-reversal symmetry spontaneously. Furthermore, they exhibit orbital frustrations and develop a chiral ordering selected by the “order-from-disorder” mechanism.

PACS numbers: 03.75.Nt, 67.85.Hj, 75.10.Jm

Bose-Einstein condensation (BEC) is a striking phenomenon of quantum many-body systems, characterized by a uniform phase that spontaneously breaks the $U(1)$ symmetry. By introducing extra degrees of freedom, novel quantum condensates with even more exotic symmetry breaking patterns and topological structures emerge. A familiar example is the superfluid ^3He phases, which is a spin-triplet p -wave Cooper pairing condensate with both spin and orbital degrees of freedom^{1,2}. It exhibits a variety of rich structures that simultaneously incorporate the symmetries of liquid crystals, magnets and scalar superfluids. Consequently, the superfluid ^3He systems possess fundamental connections with particle physics, and exemplifies fundamental concepts of modern theoretical physics³.

The rapid developments of cold atom gases provide an opportunity other than ^3He to explore exotic condensations with internal degrees of freedom. Spinor atomic gases, composed of atoms with hyperfine spins, simultaneously exhibit magnetism and superfluidity^{4–6}. Furthermore, orbital is a degree of freedom independent of spin and charge. It is originally investigated in condensed matter transition metal oxides, which plays an important role in superconductivity, metal-insulator transition, and quantum magnetism^{7,8}. Introducing orbital into cold atom gases has been theoretically investigated, which leads to unconventional BECs with complex-valued condensed wavefunction of bosons and spontaneously breaking of time-reversal symmetry^{9–16}. Excitingly, the recent experimental progress has realized the meta-stable BECs in high-orbital bands exhibiting complex-valued condensate wavefunctions at non-zero wavevectors and orbital orderings^{17–19}.

In this paper, we investigate the properties of an orbital BEC in the p -orbital bands of a cubic optical lattice. Although orbital BECs share many properties with the ferromagnetic phase in spinor BECs, there are crucial differences between them. In spinor BECs, the internal degrees of freedom of hyperfine spin degree is not coupled to the lattice. However for orbital BECs, the ordering of the orbital angular momentum comes from the atom motion within each optical site, and thus is closely related to the motion of atoms in optical lattice. As we will show, the uniqueness of the orbital degree of freedom

gives rise to a whole host of exotic phenomena, such as orbital frustration and concomitant non-collinear orbital orderings selected by the “order-from-disorder” mechanism. The selected ordering pattern exhibits an orbital angular momentum moment chirality.

The Hamiltonian of bosons pumped to the p -orbital bands of a cubic optical lattice is described by a multi-orbital Bose-Hubbard model, $H = H_t + H_{int}$,

$$H_t = \sum_{\vec{r}\mu\nu} [t_{\parallel}\delta_{\mu\nu} - t_{\perp}(1 - \delta_{\mu\nu})] \{p_{\mu,\vec{r}+a\vec{e}_{\nu}}^{\dagger} p_{\mu\vec{r}} + h.c.\},$$

$$H_{int} = \frac{U}{2} \left(n_{\vec{r}^2} - \frac{1}{3} \vec{L}_{\vec{r}}^2 \right), \quad (1)$$

where $\mu, \nu = x, y, z$ denote the orbital indices, a is the lattice constant. $p_{\mu,\vec{r}}$ ($p_{\mu,\vec{r}}^{\dagger}$) are annihilation (creation) operators for bosons at site \vec{r} in orbital μ . $n_{\vec{r}}$ is the total particle number operator and $\vec{L}_{\vec{r}}$ represents the total orbital angular momentum on site \vec{r} . t_{\parallel} and t_{\perp} describe the nearest-neighbor hopping matrix elements along the longitudinal and transverse directions, respectively. Using the terminology of chemistry, they are denoted as σ and π -bonding, respectively. Due to the odd parity of p -orbitals, t_{\parallel} and t_{\perp} are positive. The strong anisotropy of the p -band Wannier wave-function implies that $t_{\perp} \ll t_{\parallel}$. The onsite interaction term, H_{int} , reflects the Hund's type physics generalized to bosons, *i.e.*, bosons prefer to occupy complex-valued orbitals of the $p_{\hat{e}_1} + ip_{\hat{e}_2}$ type with $\hat{e}_1 \perp \hat{e}_2$. This complex-valued orbital has larger spatial extension than the real ones of p_{μ} , and thus the repulsive interactions are reduced and simultaneously the onsite orbital angular momenta are maximized^{9,13}.

We consider the orbital superfluid phase. A remarkable feature of the band structure is that the energy minima of p_{μ} ($\mu = x, y, z$)-orbitals are located at finite momenta Q_{μ} rather than at zero momentum, which are $Q_x = (\frac{\pi}{a}, 0, 0)$; $Q_y = (0, \frac{\pi}{a}, 0)$; $Q_z = (0, 0, \frac{\pi}{a})$ for the three p -orbital subbands, respectively. In the 3D cubic lattice, we will show that the onsite orbital angular momenta are no longer collinear but exhibit orbital frustrations. The single-particle states $\psi_{Q_{\mu}} = e^{iQ_{\mu} \cdot \mathbf{r}}$ ($\mu = x, y, z$) are degenerate, thus any condensate wavefunction of a linear superposition of these states,

$$|\vec{Q}\rangle = c_1|Q_x\rangle + c_2|Q_y\rangle + c_3|Q_z\rangle, \quad (2)$$

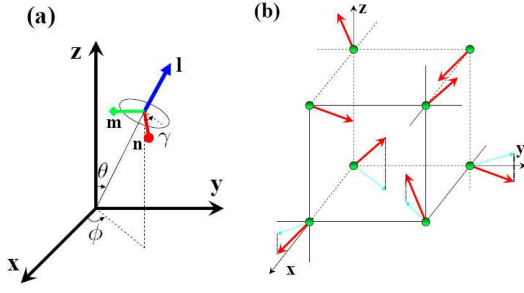


FIG. 1: (a) The $SO(3)$ manifold of the 3D p -orbital BEC order parameter in terms of Euler angles, where \mathbf{l} is the direction of the orbital angular momentum; (b) Sketch of the non-collinear orderings of orbital angular momenta in real space from Eq. (4).

yields the same kinetic energy. The complex vector $\vec{c} = (c_1, c_2, c_3)$ satisfies the normalization condition, $|\vec{c}|^2 = 1$. Next we will consider the interaction effect to lift the degeneracy and select the condensate wavefunctions.

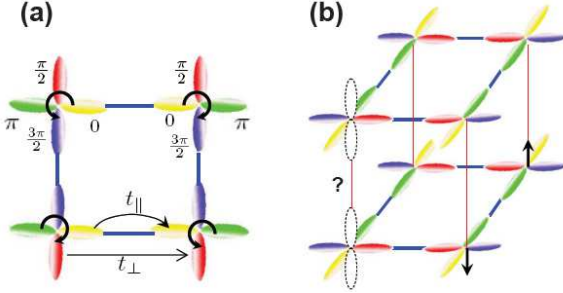


FIG. 2: (a) 2D orbital BEC in the square lattice without frustration. (b) A typical configuration of 3D orbital BEC in a cubic lattice with frustration. The thick blue bonds minimize both the transverse and parallel hopping energy, while the thin red bonds only minimize the transverse hopping energy.

The $SO(3)$ degeneracy at the classical level: At the classical level (neglecting quantum fluctuations so that the boson operator can be replaced by its average value), H_{int} is minimized if the coefficient vector \vec{c} in Eq.(2) can be expressed as $\vec{c} = \frac{1}{\sqrt{2}}(\vec{m} + i\vec{n})$, where \vec{m} and \vec{n} are two mutual perpendicular unit vectors. Transforming back into real space, for the lattice site with integer-valued coordinates $\vec{r} = (r_x, r_y, r_z)$, its onsite orbital configuration is $\frac{1}{\sqrt{2}}(p_{\hat{e}_1} + ip_{\hat{e}_2})$ with the relation

$$\begin{aligned}\hat{e}_1 &= (P_x)^{r_x} (P_y)^{r_y} (P_z)^{r_z} \vec{m}; \\ \hat{e}_2 &= (P_x)^{r_x} (P_y)^{r_y} (P_z)^{r_z} \vec{n},\end{aligned}\quad (3)$$

where $P_{x,y,z}$ are reflection operator with respect to x, y, z -axes, respectively. $\hat{e}_{1,2}$ remain orthogonal to each other, and the onsite orbital angular momentum $\vec{L}(\vec{r}) \parallel \hat{e}_1 \times \hat{e}_2$, such that \vec{L}^2 is maximized to minimize H_{int} . This denotes that at the classic level, the ground state manifold is just the configuration space of the 3D orthogonal triad

\vec{m}, \vec{n} and $\vec{l} = \vec{m} \times \vec{n}$, which is just the $SO(3)$ group space and can be expressed in terms of Euler angles (ϕ, θ, γ) , as illustrated in Fig. 1(a). Note that the multiplication of an overall $U(1)$ phase $e^{-i\varphi}$ is equivalent to the rotation of the triad around \vec{l} by the angle φ . Therefore, the $U(1)$ superfluid phase is absorbed into the $SO(3)$ group configuration space. For a given triad configuration \vec{m}_0, \vec{n}_0 and \vec{l}_0 , the corresponding real space distribution of the OAM orientation $\hat{L}(\vec{r})$ becomes

$$\hat{L}_{\vec{r}} = [(-1)^{r_y+r_z} l_x, (-1)^{r_x+r_z} l_y, (-1)^{r_x+r_y} l_z], \quad (4)$$

which is non-collinear as shown in Fig. 1(b).

Similarly to the case of frustrated magnets, this classic level degeneracy is a consequence of orbital frustration, which means that it is impossible to find an orbital configuration that simultaneously minimizes the energy of all the bonds in the lattice. To illustrate this point, let us recall the previously studied 2D case for a comparison⁹. The staggered OAM configuration in Fig. 2 (a) simultaneously minimizes both the parallel (t_{\parallel}) and transverse (t_{\perp}) hopping energies at all bonds of the square lattice, and thus there is no frustration. However, in the 3D cubic lattice, this is no longer the case. For example, if we take a similar state $|Q_{xy}\rangle = \frac{1}{\sqrt{2}}(|Q_x\rangle + i|Q_y\rangle)$, as shown in Fig. 2(b), the hopping energy of all bonds along x and y directions can be minimized, but the σ -bond along the z -direction is broken. Since the hopping Hamiltonian Eq. 1 does not preserve the $SO(3)$ symmetry, thus this classic level degeneracy should be lifted by quantum fluctuations.

Order-from-disorder In frustrated magnetism, the infinite degeneracy is usually lifted by quantum or thermal fluctuations, which is known as “order-from-disorder” mechanism^{20,21}. Below we perform the same analysis to the 3D p -orbital BECs. If we take quantum fluctuations around the mean-field values into account: $p_{\mu} = \langle p_{\mu} \rangle + \delta p_{\mu}$ and calculate the fluctuation-corrected ground state energy, quantum fluctuations lift the $SO(3)$ classical degeneracy. We consider two typical condensate configurations and compare their ground state energies (the reason to choose these two states is due to their high symmetry),

$$|Q_{diag}\rangle = \frac{1}{\sqrt{3}}(|Q_x\rangle + e^{i\frac{2\pi}{3}}|Q_y\rangle + e^{-i\frac{2\pi}{3}}|Q_z\rangle), \quad (5)$$

$$|Q_z\rangle = \frac{1}{\sqrt{2}}(|Q_x\rangle + i|Q_y\rangle). \quad (6)$$

In the state of $|Q_{diag}\rangle$, OAMs are along the body-diagonal directions, while for the state of $|Q_z\rangle$, OAMs are along the z -direction. These two configurations are degenerate at the classic level.

Here we perform the standard Bogoliubov analysis²² to calculate the zero-point motion energy of quasi-particles for these two configurations. We use the state of $|Q_{diag}\rangle$ as an example, and the calculation for $|Q_z\rangle$ is rather sim-

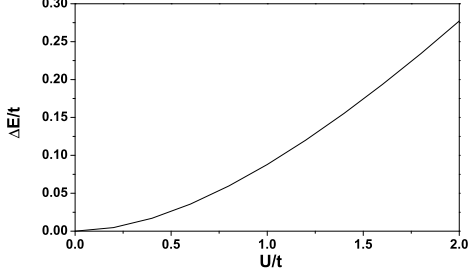


FIG. 3: The energy difference between the orbital BEC with OAM towards z -direction and body-diagonal direction $\Delta E = E_z - E_{diag}$ with $t_{\parallel} = t$, $t_{\perp} = 0.05t$ and the filling factor $n=2$.

ilar. For each p -component the order parameter is

$$\begin{aligned} \langle p_x \rangle &= (-1)^{r_x} \phi, & \langle p_y \rangle &= (-1)^{r_y} e^{\frac{2i\pi}{3}} \phi \\ \langle p_z \rangle &= (-1)^{r_z} e^{-\frac{2i\pi}{3}} \phi. \end{aligned} \quad (7)$$

To calculate the Bogoliubov spectra, we consider quantum fluctuations around the mean-field values: $p_{\mu} = \langle p_{\mu} \rangle + \delta p_{\mu}$. Expanding to the quadratic level, we arrive at

$$i\hbar \frac{\partial \Psi(\mathbf{k})}{\partial t} = \mathcal{M}(\mathbf{k}) \Psi(\mathbf{k}), \quad (8)$$

where $\Psi(\mathbf{k})$ is a 6-component vector that represents the fluctuations: $\Psi(\mathbf{k}) = [\delta\psi(\mathbf{k}), \delta\psi^{\dagger}(-\mathbf{k})]^T$, $\delta\psi(\mathbf{k}) = [\delta p_x(\mathbf{k}), \delta p_y(\mathbf{k} + \mathbf{Q}_{xy}), \delta p_z(\mathbf{k} + \mathbf{Q}_{xz})]$, $\mathbf{Q}_{xy} = (\pi, \pi, 0)$, and $\mathbf{Q}_{xz} = (\pi, 0, \pi)$. $\mathcal{M}(\mathbf{k})$ is a 6×6 matrix as

$$\mathcal{M}(\mathbf{k}) = \begin{bmatrix} \mathcal{H}(\mathbf{k}) & \Delta(\mathbf{k}) \\ -\Delta^{\dagger}(\mathbf{k}) & -\mathcal{H}(-\mathbf{k}) \end{bmatrix},$$

in which both \mathcal{H} and $\Delta(\mathbf{k})$ are 3×3 matrices:

$$\begin{aligned} \mathcal{H}(\mathbf{k}) &= \begin{bmatrix} \epsilon_{\mathbf{k}}^x + 2w & -w & -w \\ -w & \epsilon_{\mathbf{k}+\mathbf{Q}_{xy}}^y + 2w & -w \\ -w & -w & \epsilon_{\mathbf{k}+\mathbf{Q}_{xz}}^z + 2w \end{bmatrix}, \\ \Delta(\mathbf{k}) &= \begin{bmatrix} w & e^{i\frac{2\pi}{3}} w & e^{-i\frac{2\pi}{3}} w \\ e^{-i\frac{2\pi}{3}} w & w e^{-i\frac{2\pi}{3}} & w \\ w e^{-i\frac{2\pi}{3}} & w & w e^{i\frac{2\pi}{3}} \end{bmatrix}, \end{aligned} \quad (9)$$

where $w = \frac{2}{3}u\phi_{dg}^2$; $\epsilon_{\mathbf{k}}^{\mu} = 2 \sum_{\nu} [t_{\parallel} \delta_{\mu\nu} - t_{\perp} (1 - \delta_{\mu\nu})] \cos(k_{\nu}a)$ is the single particle energy spectrum for the μ band boson. The self-consistent equation to determine value of ϕ_{dg} is

$$n = |\phi_{dg}|^2 - \frac{1}{2} + \frac{1}{2} \sum_{\mathbf{k}} \frac{\bar{\epsilon}(\mathbf{k}) + 2U|\phi_{dg}|^2}{\sqrt{\bar{\epsilon}(\mathbf{k})(\bar{\epsilon}(\mathbf{k}) + 4U|\phi_{dg}|^2)}} \quad (10)$$

where $\bar{\epsilon}(\mathbf{k}) = (\epsilon_{\mathbf{k}}^x + \epsilon_{\mathbf{k}+\mathbf{Q}_{xy}}^y + \epsilon_{\mathbf{k}+\mathbf{Q}_{xz}}^z)/3$, and n is the filling factor. The contribution from the zero point motion energy to the ground state energy can be written as

$$E_{diag}^0 = -3Un_c^2 - Un_c - t + \frac{1}{2} \sum_{\mathbf{k}} \sqrt{\bar{\epsilon}(\mathbf{k})(\bar{\epsilon}(\mathbf{k}) + 4Un_c)}$$

where $n_c = |\phi_{dg}|^2$, $t = t_{\parallel} + 2t_{\perp}$. Performing the same process, we obtain the correction for $|Q_z\rangle$, and the difference $\Delta E = E_z - E_{diag}$ is plotted in Fig. 3.

For fixed parameters $U, t_{\parallel}, t_{\perp}$ and boson density n , the energy of $|Q_{diag}\rangle$ is always lower than that of $|Q_z\rangle$ i.e., $\Delta E = E_z - E_{diag} > 0$, which means that orbital BECs in a cubic lattice prefer to develop OAM moments along the body-diagonal directions. Such a configuration has a high symmetry, and all the bonding strengths are uniform in the lattice. In comparison, all the σ -bonds along the z -direction are broken in the state of $|Q_z\rangle$. This “order-from-disorder” phenomenon is another feature that distinguishes orbital BECs from spinor BECs.

Spontaneous chiral orbital order: In condensed matter physics, the presence of spin chirality plays important roles in frustrated magnetism²³, doped Mott-insulators²⁴, and the anomalous quantum Hall effect²⁵. Here, we find that the orbital BECs in Eq. (5) spontaneously develops a chiral orbital angular momentum ordering. Eq. (5) has a time-reversal partner as

$$|Q'_{diag}\rangle = \frac{1}{\sqrt{3}}(|Q_x\rangle + e^{-i\frac{2\pi}{3}}|Q_y\rangle + e^{i\frac{2\pi}{3}}|Q_z\rangle). \quad (11)$$

The orbital angular momentum orderings of Eq. 5 and Eq. 11 are plotted in Fig. 4. To distinguish the chirality between $|Q_{diag}\rangle$ and $|Q'_{diag}\rangle$, we define a nonzero chirality (similar to the case of chiral spin liquid²⁴):

$$\chi_{ijk} = \vec{l}_i \cdot (\vec{l}_j \times \vec{l}_k), \quad (12)$$

where ijk denotes three sites of the four corners of the plaquette in a clockwise direction, as shown in Fig. 4 (c). In contrast to the chiral spin liquid²⁴ (where $\langle \vec{S} \rangle = 0, \chi \neq 0$) and the spinor BEC (where $\langle \vec{S} \rangle \neq 0, \chi = 0$), the orbital BEC in our case simultaneously exhibits non-vanishing orbital order and orbital chirality order ($\langle \vec{l} \rangle \neq 0, \chi \neq 0$).

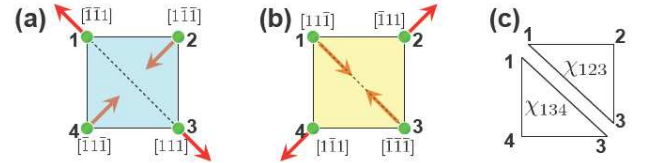


FIG. 4: Ordering patterns in a plaquette for (a) $|Q^1_{diag}\rangle$ and (b) $|Q^2_{diag}\rangle$ with opposite chirality; (c) Definition of the chirality in a plaquette.

Excitations: Now we discuss the collective modes and elementary excitations of the orbital BECs in the state of $|Q_{diag}\rangle$. From the EOM Eq. (8), we obtain the collective modes by diagonalizing the matrix \mathcal{M} . In the long-wavelength limit ($k \rightarrow 0$), we find that there are three modes: (1) the gapless Goldstone mode corresponding to the fluctuation of the superfluid phase of the orbital BECs with linear dispersion, $\omega_1(\mathbf{k}) \approx \sqrt{2U|\phi|^2(2t_{\perp} + t_{\parallel})}|\mathbf{k}|$, (2) the orbital wave mode corresponding to the fluctuation of the OAM around its

ground state directions, $\omega_2(\mathbf{k}) \approx \frac{2t_{\perp} + t_{\parallel}}{2}k^2$, (3) the gapped mode, which describes orbital excitations corresponding to the flipping of orbital angular momenta, $\omega_3(\mathbf{k}) \approx \frac{2t_{\perp} + t_{\parallel}}{2}k^2 + 2U|\phi|^2$.

Ginzburg-Landau (GL) free energy: To better understand the various phases in orbital BECs, we first identify the order parameters of the different phases. The orbital BECs are characterized by both superfluidity with order parameters φ_{μ} ($\mu = x, y, z$) and orbital order \vec{L} , which is a 3-component real vector L_{μ} (after the transformation defined in Eq. 4, the non-collinear order can be transformed into a spatially uniform one). Notice that these two different orders are not necessarily simultaneously present. To clarify this point, we construct a GL free energy in terms of χ_{μ} and \vec{L} :

$$\mathcal{F} = \sum_{\mu} r|\varphi_{\mu}|^2 + u|\varphi_{\mu}|^4 + r'|\vec{L}|^2 + u'(|\vec{L}|^2)^2 + \sum_{\mu\nu} v|\varphi_{\mu}|^2|\varphi_{\nu}|^2 - g\varepsilon^{\lambda\mu\nu}i(\varphi_{\mu}^*\varphi_{\nu} - \varphi_{\nu}^*\varphi_{\mu})L_{\lambda} \quad (13)$$

the last term is the minimal coupling between the superfluid and orbital orders and the parameters g , u' , u are positive in our case. For the the orbital BEC in Eq. 5, \vec{L} is along the body-diagonal direction and the free energy Eq.13 can be simplified to

$$\mathcal{F} = r_0\phi^2 + u_0\phi^4 + r'_0l^2 + u'_0l^4 - g_0\phi^2l + \dots \quad (14)$$

The free energy \mathcal{F} describes both thermodynamic phase transitions which are driven by temperature and quantum phase transitions where the parameters are a function of U/t . By minimizing the free energy in Eq. (14), we find that: for $r'_0 < 0$ and $r_0 < \sqrt{-\frac{g_0^2 r'_0}{2u'_0}}$, both ϕ and l are non-zero at the free energy minima, which corresponds to orbital BECs with both superfluidity and orbital order; for $r'_0 < 0$ and $r_0 > \sqrt{-\frac{g_0^2 r'_0}{2u'_0}}$, $\phi = 0$ while $l \neq 0$, so in this case the single particle condensations are suppressed by thermal or quantum fluctuations while the orbital order is preserved; for $r'_0 > 0$ and $r_0 > 0$, both ϕ and l are zero, which means that both the superfluidity and orbital order have been destroyed, corresponding to the high temperature normal phases or featureless Mott insulator at zero temperature.

Experimental detection: Next we discuss the experimental detection of orbital ordering and unconventional

BEC characterized by the ordering parameters in Eq.(7). The condensate wavefunction in Eq.(11) is a superposition of the single-particle states of three condensate momenta with equal weights but different phases, as a consequence, the time-of-flight (TOF) image will exhibits three peaks with the same height in the points corresponding to $\mathbf{Q}_{x,y,z}$. However, TOF images only provide the single-particle density distribution in momentum space, while the key information about the relative phase between different condensate components is lost during TOF. To measure the phase difference $e^{\pm i\frac{2\pi}{3}}$ defined in Eq.(7), the phase sensitive detections proposed recently can be employed²⁶. Impulsive Raman operations can be applied to couple any two among the three components at different momenta. The relative phase information can be read out from the interference pattern from the TOF imaging.

At last, we will briefly discuss the orbital BECs in higher bands. Recently, an unconventional BEC in the f -band of a bipartite optical square lattice has been observed experimentally¹⁹. Surprisingly, d -band BECs have also been observed in a distinct field: the exciton-polariton condensate²⁷. Orbital BECs in the p -band of 3D optical lattice have three components (p_x , p_y , p_z), and the interactions favor a ferro-orbital state with OAM $L = 1$, which makes it similar to the ferromagnetic phase of spinor BECs with $F = 1$. Analogously, orbital BECs in higher bands behave similarly to spinor BECs with higher spin^{28–31}. Apparently for orbital BECs in higher bands, the geometry and symmetry group of the order parameters is far more complex and may give rise to richer physics.

In conclusion, we investigate the frustrated orbital ordering of p -band unconventional BECs in the cubic lattice, and we find that the uniqueness of the orbital degree of freedom gives rise to a lot of interesting phenomena that absent in the spinor BECs and superfluid³ He, such as orbital frustration and concomitant non-collinear orbital orderings selected by the “order-from-disorder” mechanism. The chiral symmetry breaking and the elementary excitations have also been discussed.

Z. C. and C. W. are supported by the NSF DMR-1105945 and the AFOSR-YIP program. Y.W. gratefully acknowledges the support of Wuhan University through the New Faculty Start-Up Grant.

* Electronic address: zcai@physics.ucsd.edu

† Electronic address: yu.wang@whu.edu.cn

¹ A. J. Leggett, Rev. Mod. Phys. **47**, 331 (1975).

² D. Vollhardt and P. Wölfle, *The superfluid phases of helium 3* (Taylor & Francis, London, 1990).

³ G. E. Volovik, *The Universe in a Helium Droplet* (Oxford University Press, Oxford, 2003).

⁴ D. M. Stamper-Kurn, M. R. Andrews, A. P. Chikkatur, S. Inouye, H.-J. Miesner, J. Stenger, and W. Ketterle, Phys. Rev. Lett. **80**, 2027 (1998).

⁵ J. Stenger, S. Inouye, D. Stamper-Kurn, H.-J. Miesner, A. Chikkatur, and W. Ketterle, Nature **396**, 345 (1998).

⁶ T.-L. Ho, Phys. Rev. Lett. **81**, 742 (1998).

⁷ M. Imada, A. Fujimori, and Y. Tokura, Rev. Mod. Phys.

- 70**, 1039 (1998).
- ⁸ Y. Tokura and N. Nagaosa, *Science* **288**, 462 (2000).
 - ⁹ W. V. Liu and C. Wu, *Phys. Rev. A* **74**, 13607 (2006).
 - ¹⁰ A. Isacsson and S. M. Girvin, *Phys. Rev. A* **72**, 053604 (2005).
 - ¹¹ A. B. Kuklov, *Phys. Rev. Lett.* **97**, 110405 (2006).
 - ¹² C. Wu, W. V. Liu, J. E. Moore, and S. Das Sarma, *Phys. Rev. Lett.* **97**, 190406 (2006).
 - ¹³ C. Wu, *Modern Physics Letters B* **23**, 1 (2009).
 - ¹⁴ Z. Cai and C. Wu, *Phys. Rev. A* **84**, 033635 (2011).
 - ¹⁵ X. Li, Z. Zhang, and W. V. Liu, *Phys. Rev. Lett.* **108**, 175302 (2012).
 - ¹⁶ A. Collin, J. Larson, and J. P. Martikainen, *Phys. Rev. A* **81**, 023605 (2010).
 - ¹⁷ T. Mueller, S. Foelling, A. Widera, and I. Bloch, *Phys. Rev. Lett.* **99**, 200405 (2007).
 - ¹⁸ G. Wirth, M. Ölschläger, and A. Hemmerich, *Nature Physics* **7**, 147 (2011).
 - ¹⁹ M. Ölschläger, G. Wirth, and A. Hemmerich, *Phys. Rev. Lett.* **106**, 015302 (2011).
 - ²⁰ C. L. Henley, *Phys. Rev. Lett.* **62**, 2056 (1989).
 - ²¹ A. Chubukov, *Phys. Rev. Lett.* **69**, 832 (1992).
 - ²² D. van Oosten, P. van der Straten, and H. T. C. Stoof, *Phys. Rev. A* **63**, 053601 (2001).
 - ²³ D. Grohol, K. Matan, J.-H. Cho, S.-H. Lee, J. W. Lynn, D. G. Nocera, and Y. S. Lee, *Nature Materials* **4**, 323 (2005).
 - ²⁴ X. G. Wen, F. Wilczek, and A. Zee, *Phys. Rev. B* **39**, 11413 (1989).
 - ²⁵ Y. Taguchi, Y. Oohara, H. Yoshizawa, N. Nagaosa, and Y. Tokura, *Science* **291**, 2573 (2001).
 - ²⁶ Z. Cai, L. M. Duan and C. Wu, arXiv:1110.3021, (2011);
 - ²⁷ N. Y. Kim, K. Kusudo, C. Wu, N. Masumoto, C. Schneider, S. Höling, N. Kumada, L. Worschech, A. Forchel, and Y. Yamamoto, *Nature Physics* **7**, 681 (2011).
 - ²⁸ R. Barnett, A. Turner, and E. Demler, *Phys. Rev. Lett.* **97**, 180412 (2006).
 - ²⁹ M. Koashi and M. Ueda, *Phys. Rev. Lett.* **84**, 1066 (2000).
 - ³⁰ C. V. Ciobanu, S.-K. Yip, and T.-L. Ho, *Phys. Rev. A* **61**, 033607 (2000).
 - ³¹ L. Santos and T. Pfau, *Phys. Rev. Lett.* **96**, 190404 (2006).